COMMUNICATION

Isotopic substitution affects excited state branching in a DNA duplex in aqueous solution

Received 00th February 20xx,
Accepted 00th February 20xx

DOI: 10.1039/x0xx00000x

Yuyuan Zhang,†[a] Kimberly de La Harpe,†[b] Forrest R. Kohl[a] and Bern Kohler*[a]

Changing the solvent from H_2O to D_2O dramatically affects the branching of the initial excited electronic states in an alternating G·C DNA duplex into two distinct decay channels. The slower, multisite PCET channel that deactivates more than half of all excited states in D_2O becomes six times weaker in H_2O.

UV excitation of DNA strands in aqueous solution at room temperature produces excited electronic states with lifetimes that are orders of magnitude longer than ones observed in single nucleotides under the same conditions.[1] These unusual excitations, their nature, and dynamics are of great interest as slower energy relaxation could potentially diminish DNA's intrinsic resistance to photodamage. Growing evidence indicates that the long-lived excited states in DNA strands are intrastrand charge transfer (CT) states formed by photoinduced electron transfer.[2-6] The requirement that the bases must be π-π stacked with one another in order to form the CT states is seen clearly in experiments on single-stranded nucleic acids.[7]

In DNA duplexes, stacked bases on one strand are joined by hydrogen bonds to complementary bases on a second strand. This architecture allows nucleobases that function as electron donors and acceptors in excited states to simultaneously interact as proton donors and acceptors. Furthermore, the short distances in DNA between interacting nucleobases allow photoinduced electron transfer (ET) and proton transfer (PT) reactions to proceed on the ultrafast time scales that characterise excited-state decay in DNA. For these reasons, couplings between ET and PT have figured prominently in paradigms for nonradiative decay by DNA excited states.[1, 8-10]

These circumstances make DNA duplexes very promising for fundamental studies of photoinduced proton-coupled electron transfer (P-PCET). P-PCET is a highly attractive route to chemicals of great interest in solar fuels and photocatalysis,[11, 12] but the role that P-PCET plays in the ultrafast nonradiative decay of excited states in systems like DNA is not widely appreciated.

DNA is advantageous for P-PCET studies for several reasons. First, the base sequence can be readily varied and non-canonical bases and base-pairing motifs can be introduced. Second, structures are often known with atomic resolution, allowing the distances between charge donors and acceptors to be determined precisely. Third, photoexcitation of DNA initially produces delocalized excited states or excitons due to electronic couplings among neighbouring bases in this multichromophoric molecule.[13] To date, studies of P-PCET have focused on systems in which a single molecular absorber is excited.[14] Although photosystem I and II famously make use of delocalized excitons in their light-harvesting proteins for capturing photon energy, the PCET events of interest take place subsequently and involve thermally relaxed states.[15] DNA thus provides an opportunity to investigate how the ultrafast (de)localization of excitation energy affects P-PCET.

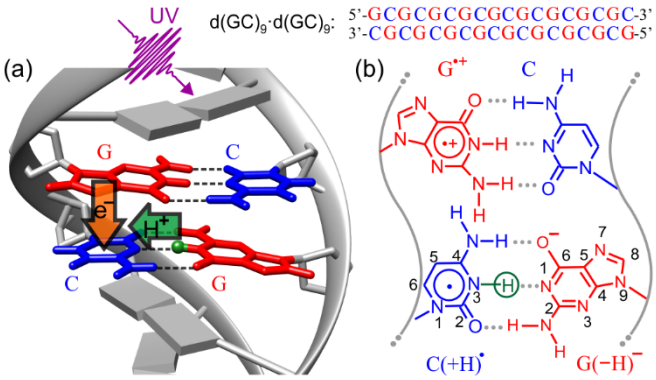

Fig. 1. Two G·C base pairs in an alternating $d(GC)_9 \cdot d(GC)_9$ duplex (sequence at top). (a) Arrows show the electron and proton transfers after UV excitation proposed in ref. 10, which yield the transient PCET state (b) with all labile protons shown. The structure in (a) was drawn using the UCSF Chimera package.[16]

Here, we investigate the effect of isotopic substitution on the excited-state dynamics of a $d(GC)_9 \cdot d(GC)_9$ duplex by broadband femtosecond UV-visible transient absorption (TA) spectroscopy. UV excited states of this frequently studied model duplex have been proposed to decay via a multisite PCET mechanism in D_2O solution.[10, 17, 18] In particular, a transient excited state, formed by intrastrand ET and interstrand PT (Fig. 1a), was detected through vibrational marker bands of the three nucleobases affected (Fig. 1b)

[a] *Department of Chemistry and Biochemistry, The Ohio State University, 100 West 18th Avenue, Columbus, Ohio 43210, United States.*
[b] *Department of Physics, United States Air Force Academy, U.S. Air Force Academy, Colorado 80840, United States.*
† Authors contributed equally to this work.
Electronic Supplementary Information (ESI) available. Experimental methods; steady-state spectra; fitting parameters for GSB traces, broadband TA data for G, C, $G^{\bullet+}$ and $G(-H)^{\bullet}$. See DOI: 10.1039/x0xx00000x

using time-resolved infrared (TRIR) spectroscopy.[10, 17, 18] Henceforth, we will refer to this state, which has not yet been detected in H_2O solution, as the PCET state.

TA signals observed for this model DNA duplex decay biexponentially with a fast component with a time constant of several picoseconds and a slower one lasting tens of picoseconds.[10, 19] In ref 17, the slower component was assigned to decay of the PCET state via rate-limiting intrastrand back ET followed by ultrafast interstrand PT, but the shorter lifetime component has not been assigned. Consequently, it is not understood how the PCET state forms and whether other excited states are present. We report here that the short-lived state is not a precursor to the long-lived PCET state, but represents a parallel decay channel that is strongly enhanced in H_2O at the expense of the PCET channel.

Measurements on the $d(GC)_9{\cdot}d(GC)_9$ duplex in H_2O and D_2O solutions were carried out in a 50 mM phosphate buffer solution containing 100 mM NaCl. In D_2O, the five labile protons explicitly shown in each GC base pair in Fig. 1b are replaced by deuterons. The B-form $d(GC)_9{\cdot}d(GC)_9$ duplex (see Fig. S1 in Supporting Information (SI) for sample characterization) was excited at 265 nm, and the ensuing excited-state dynamics were monitored by the femtosecond TA technique as described in the ESI. All measurements in H_2O and D_2O were performed in back-to-back experiments in which the sample absorbance and all excitation conditions were held constant in order to form identical numbers of initial excited states in each sample. Because the average number of excitations per duplex molecule is estimated to be 0.4 (see the ESI), we interpret the dynamics in terms of single, independent excitations.

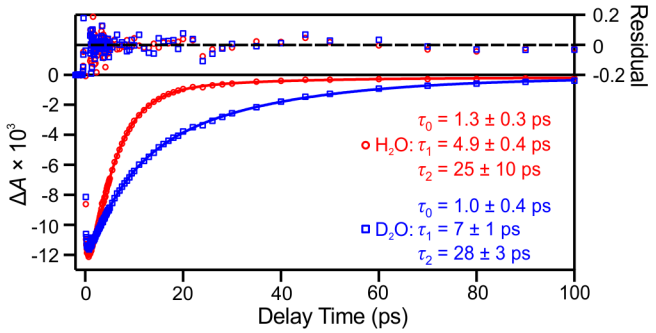

Fig. 2. Ground-state bleach recovery traces monitored at 250 nm following 265 nm excitation of the $d(GC)_9{\cdot}d(GC)_9$ duplex in H_2O (red) and in D_2O (blue). The fit parameters are included for convenience, and the fit residual is shown on top of the panel.

We began by investigating the TA signals of $d(GC)_9{\cdot}d(GC)_9$ in H_2O and D_2O with excitation at 265 nm and probing at 250 nm, as de La Harpe et al.[19] did a decade ago. As in that earlier study, we observe ground state bleaching (GSB) signals from the D_2O sample that decay biexponentially over most of the delay time window (Fig. 2). However, in H_2O solution, what had been described as a monoexponential decay in ref. 19 is clearly seen using the superior signal-to-noise ratio of our current spectrometer to include a weak, long-lived component beyond 20 ps. A weak sub-picosecond component is also seen at short times.

The signals in Fig. 2 were fit to a triexponential function plus a constant offset between 1 ps and 450 ps. This choice of function accounts for a weak subpicosecond component present at $t < 1$ ps, which has an amplitude opposite in sign to the other components. The fitting parameters are tabulated in Table S1. Note that fitting the signals to a biexponential function plus an offset as was done in ref. 19 gives a poor fit (Fig. S2, Table S2).

The τ_2 lifetimes in H_2O and D_2O agree within experimental uncertainty, while the lifetime of the fast component (τ_1) in D_2O (7 ± 1 ps) is slightly greater than in H_2O (4.9 ± 0.4 ps). The lifetimes in D_2O agree very well with ones determined in previous TRIR experiments in the same solvent on $d(GC)_9{\cdot}d(GC)_9$ (τ_1 = 7.4 ± 0.4 ps, τ_2 = 31 ± 1 ps),[17] and on poly(dGdC)·poly(dGdC) (τ_1 = 7 ± 1 ps, τ_2 = 30 ± 4 ps).[20]

Next, TA measurements with broadband probing from 320 nm to 630 nm were carried out on H_2O and D_2O solutions of $d(GC)_9{\cdot}d(GC)_9$ (Fig. 3a,b). The use of transient electronic spectroscopy allows us to investigate H/D isotope effects, which are difficult to study by TRIR spectroscopy due to the poor mid-IR transmission of H_2O. The TA spectra in both solvents are nearly featureless between 450 nm and 630 nm, but show a very weak maximum near 550 nm. The spectra rise sharply below 450 nm and a band at 390 nm is observed in both solvents. The latter feature is not seen in TA spectra of the G or C monomers (Fig. S3a,b) or in the signal (estimated) from their equimolar mixture (Fig. S3c). The transient spectra thus arise from excited states that are unique to π-stacked and/or H-bonded assemblies in the duplex.

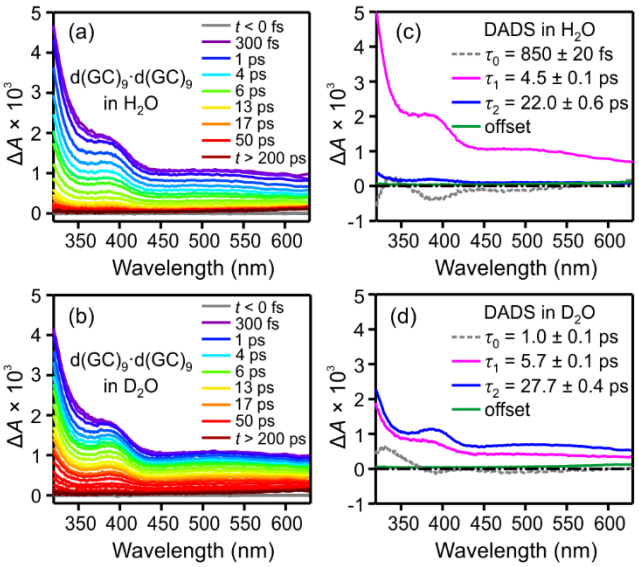

Fig. 3. Broadband UV-visible TA spectra of $d(GC)_9{\cdot}d(GC)_9$ in H_2O (a) and D_2O (b), and the decay-associated difference spectra obtained from global fitting the TA data for the H_2O (c) and D_2O (d) solutions.

After 1 ps, the signals decay monotonically at all probe wavelengths. Satisfactory global fits to the measured absorbance change (ΔA) in both solvents from 1 ps to 450 ps are obtained using eq. 1,

$$\Delta A = A_0(\lambda)e^{-t/\tau_0} + A_1(\lambda)e^{-t/\tau_1} + A_2(\lambda)e^{-t/\tau_2} + A_3(\lambda), \qquad (1)$$

where τ_i and $A_i(\lambda)$ are the time constant and the decay-associated difference spectrum ($DADS_i$), respectively, of the ith decay component. In both solvents, the A_3 term was needed to fit the signals at $t > 100$ ps. This constant component is assigned to two-photon ionization of the solvent.

Global fits to the broadband data in H_2O yields lifetimes of 850 ± 20 fs, 4.5 ± 0.1 ps, and 22.0 ± 0.6 ps for τ_0, τ_1, and τ_2, respectively. Globally fitting the signals in D_2O yields lifetimes of 1.0 ± 0.1 ps, 5.7

± 0.1 ps and 27.7 ± 0.4 ps. All lifetimes agree well with ones from the GSB recovery signals in Fig. 2. $DADS_i$ for i = 0 – 3 are shown in Fig. 3c,d.

The relative simplicity of the dynamics is surprising given the many transient species possible in a thermally disordered supramolecular assembly of 36 nucleobases. In addition to excited states localized on C or G, there could be a variety of intra- and interstrand CT states.[9] Proton transfer is nominally favourable according to ground-state estimates in one or both radical ion base pairs formed by intrastrand ET from G to C.[10] Excited states like these could form and decay on different time scales, potentially resulting in complex dynamics. In spite of this, the signal decay after 5 ps is due to just two intermediates according to the results presented here and in previous TRIR experiments.[10]

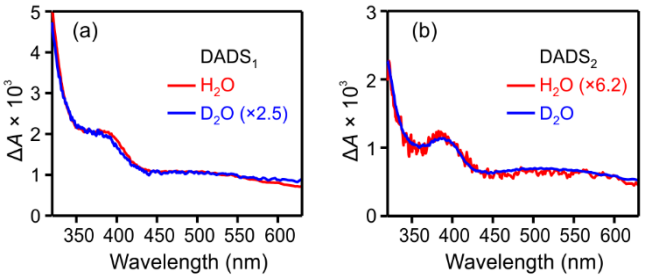

Fig. 4. Comparison of the DADS of the fast (a) and slow (b) components in H_2O (red) and D_2O (blue) after scaling by the factors shown.

We first discuss the spectral features of $DADS_1$ and $DADS_2$ and then their amplitudes. We focus on $DADS_1$ and $DADS_2$ as they account for the signal dynamics several ps after excitation once the fastest component has decayed. After scaling, $DADS_1$ from the H_2O solution agrees quantitatively with $DADS_1$ from the D_2O solution (Fig. 4a). The $DADS_2$ in both solvents also agree after scaling (Fig. 4b). Importantly, the scaling factors shown in Fig. 4 indicate that the amplitudes of $DADS_1$ and $DADS_2$ in H_2O are 2.5 times higher and 6.2 times lower compared to those in D_2O, respectively. Very similar ratios are observed for the amplitudes of the GSB traces (Table S1).

Subtle, but reproducible differences are seen between $DADS_1$ and $DADS_2$. Both exhibit a feature near 390 nm, but a shoulder is seen in $DADS_1$, whereas $DADS_2$ shows a clear peak with a distinct maximum. $DADS_2$ agrees well with the spectrum measured after two-photon ionization of 5'-GMP (Fig. S4), which in turn matches a literature spectrum of $G^{\bullet+}$.[21] The shoulder at 390 nm in $DADS_1$ appears more similar to the neutral G radical, $G(-H)^{\bullet}$, produced by deprotonation of the radical cation (Fig. S4). These two radicals are known to have very similar absorption spectra,[21] but the subtle differences seen in the literature match the ones measured here.

The presence of $G^{\bullet+}$ in the D_2O solution is consistent with the PCET state (Fig. 1b), but the other species seen in the TRIR spectra, $C(+D3)^{\bullet}$ and $G(-D1)^{-}$ are difficult to detect in the window probed by our broadband UV-visible spectra. Deprotonated G absorbs negligibly above 300 nm (Fig. S5) and thus cannot contribute to the TA signals in Fig. 3. The neutral C radical, $C(+H3)^{\bullet}$ or $C(+D3)^{\bullet}$, likely absorbs only weakly in the visible,[22, 23] but this is difficult to isolate from $G^{\bullet+}$, which also absorbs in this region.[21] The lack of clear signatures for $C(+D3)^{\bullet}$ and $G(-D1)^{-}$ prevent definitive identification of the PCET state solely from the broadband UV-visible measurements. However, the similar lifetime seen here and in the TRIR experiments in D_2O (27.7 ± 0.4 ps vs. 31 ± 1 ps[17]) indicate that the underlying state is the same.

The same state is also seen in H_2O and D_2O at long times based on the similar τ_2 lifetimes (~25 ps) and agreement of the scaled $DADS_2$ (Fig. 4). At long times, there is much less signal in H_2O than in D_2O as can be seen from a comparison of the signals at 50 ps (Fig. 3a,b). Because this common final state has similar lifetimes in both solvents, the signal in H_2O must be weaker at all times.

Each transient species detected in a TA experiment contributes to the signal through the product of its population multiplied by its absorption cross section (minus that of the initial absorber). Because H/D substitution does not change absorption cross sections, the weaker signal seen in H_2O is an indication that the population of this state is lower than in D_2O. Precisely how much lower can be quantified because the equality of the absorption cross sections upon H/D substitution implies that the ratio of the signal amplitudes is equal to the population ratio. Thus, the ratio of 6.2 indicates that the population of the longest-living state, or PCET state, is 6.2 times lower in H_2O. The ratio of A_2 for the GSB trace in D_2O to its value in H_2O is 6.4 (Table S1), leading to the same conclusion.

A further insight from this analysis is that the state responsible for the τ_1 component cannot decay solely to the long-time PCET state, ruling out a simple sequential decay mechanism. The lack of a precursor-successor relationship between the states responsible for $DADS_1$ and $DADS_2$ indicates that branching occurs to parallel decay pathways. A simple, but by no means unique mechanism is that the 5 ps lifetime characterises a decay pathway that operates in parallel to the PCET channel. The branching between these channels is not resolved in our measurements or could be taking place during the dynamics captured by τ_0. Experiments performed with higher time resolution could provide new insights.

The precise nature of the second pathway that operates in parallel to the decay of the PCET state is uncertain. In ref. 18, it was suggested that this state could be due to the electron-driven PT mechanism discussed in ref. 8. The strong resemblance of $DADS_1$ to the $G(-H)^{\bullet}$ radical is consistent with such a channel, but we caution that other explanations are possible. For example, the somewhat broader band seen at 390 nm in $DADS_1$ could be assigned to vibrationally hot $G^{\bullet+}$.

The absorption feature at 390 nm, whether it arises from $G(-H)^{\bullet}$ or $G^{\bullet+}$, is plainly visible in the earliest transient spectra in our measurements (Fig. 3a,b), indicating that the radical forms faster than the time resolution of these measurements (~200 fs). The prompt detection of a G radical by ultrafast electronic spectroscopy complements previous TRIR measurements that support rapid intrastrand ET in DNA strands.[5]

Because photoexcitation of DNA strands results in charge redistribution on an ultrafast time scale, the ensuing decay dynamics are likely to be shaped by factors important in other ultrafast PCET systems. Some key issues have been pinpointed in recent studies of the *p*-nitrophenylphenol/*tert*-butylamine complex, a model system for P-PCET.[24-26] For example, solvent dynamics can greatly influence the rate of PT in the initial CT state.[24, 26] Solvation dynamics unfold in H_2O and D_2O on the time scale of hundreds of fs,[27] or fast enough to influence branching to a PCET state. How quickly the solvent can stabilize a charged intermediate, such as a PCET state, could influence branching to a competing decay channel that involves intermediates with a lesser degree of charge separation, such as the neutral radicals postulated in the electron-driven PT mechanism.[8]

It is important, however, to consider not just solvent effects, but also ones due to solute deuteration. QM/MM nonadiabatic dynamics simulations on the above phenol-amine complex predict

that the fraction of population undergoing PT on the different electronic states is sensitive to H/D substitution of the solute.[26] As shown in Fig. 1b, H/D exchange occurs at five sites per GC base pair in our duplex. Vibronic couplings among electron-proton states of the donor and acceptor that govern transitions among electronic states depend sensitively on the vibrational wave function overlap.[11, 28, 29] Because energy splittings between vibronic states are smaller for deuterium than for hydrogen, these overlaps can vary dramatically depending on the vibrational excess energy in the initial vs. final state.[11, 28, 29]

Analysis of nonequilibrium effects on ultrafast PCET reactions reveals that deuteration does not always increase excited state lifetimes.[11,28,29] In our measurements, τ_1 and τ_2 do increase modestly by a factor of ~1.3 in D_2O vs. H_2O, but the dominant effect of H/D substitution is on the branching to these distinct channels. The isotopic sensitivity of this branching suggests to us that both decay channels may involve PCET, although an assignment for the faster ~5 ps channel requires additional experimental and theoretical work.

In summary, we have reported femtosecond broadband TA signals at near UV-visible probe wavelengths on a DNA duplex for the first time. Through much of the time window from ~4 ps to 500 ps, the signals provide evidence of just two components that arise from two spectroscopic intermediates. Analysis of the signals indicates that the short-lived intermediate is not the precursor of the long-lived one, which was previously assigned to a PCET excited state. Instead, the τ_1 and τ_2 components appear to be separate populations reached by branching that is complete within ~1 ps from a common precursor state. The multisite PCET mechanism, which deactivates more than half of all excited states in D_2O, is almost undetectable in H_2O. The isotopic sensitivity of excited-state branching may be a general phenomenon observable in other supramolecular systems that support multiple P-PCET pathways, revealing rich dynamics not found in P-PCET systems with only a single molecular absorber.

The work at OSU was supported by the U.S. National Science Foundation (CHE-1800471). K.d.L.H. thanks USAFA for support during a sabbatical leave. We thank Prof. James T. Hynes (U. of Colorado and ENS, France), Prof. Damien Laage (ENS, France), Dr. Fabrizio Santoro (National Research Council, Italy), Dr. Lara Martínez-Fernández (IBB-CNR, Italy) and Dr. Roberto Improta (IBB-CNR, Italy) for helpful discussions.

Conflicts of interest

There are no conflicts to declare.

Notes and references

1. C. E. Crespo-Hernández, B. Cohen and B. Kohler, *Nature*, 2005, **436**, 1141.
2. G. W. Doorley, M. Wojdyla, G. W. Watson, M. Towrie, A. W. Parker, J. M. Kelly and S. J. Quinn, *J. Phys. Chem. Lett.*, 2013, **4**, 2739.
3. M. C. Stuhldreier and F. Temps, *Faraday Discuss.*, 2013, **163**, 173.
4. D. B. Bucher, B. M. Pilles, T. Carell and W. Zinth, *Proc. Nat. Acad. Sci. USA*, 2014, **111**, 4369.
5. Y. Zhang, J. Dood, A. A. Beckstead, X.-B. Li, K. V. Nguyen, C. J. Burrows, R. Improta and B. Kohler, *Proc. Nat. Acad. Sci. USA*, 2014, **111**, 11612.
6. Y. Zhang, J. Dood, A. A. Beckstead, X.-B. Li, K. V. Nguyen, C. J. Burrows, R. Improta and B. Kohler, *J. Phys. Chem. B*, 2015, **119**, 7491.
7. J. Chen and B. Kohler, *J. Am. Chem. Soc.*, 2014, **136**, 6362.
8. A. L. Sobolewski and W. Domcke, *Phys. Chem. Chem. Phys.*, 2004, **6**, 2763.
9. C. Ko and S. Hammes-Schiffer, *J. Phys. Chem. Lett.*, 2013, **4**, 2540.
10. Y. Zhang, K. de La Harpe, A. A. Beckstead, R. Improta and B. Kohler, *J. Am. Chem. Soc.*, 2015, **137**, 7059.
11. S. Hammes-Schiffer, *J. Am. Chem. Soc.*, 2015, **137**, 8860.
12. J. C. Lennox, D. A. Kurtz, T. Huang and J. L. Dempsey, *ACS Energy Lett.*, 2017, **2**, 1246.
13. L. M. Nielsen, S. V. Hoffmann and S. B. Nielsen, *Photoch. Photobio. Sci.*, 2013, **12**, 1273.
14. O. S. Wenger, *Acc. Chem. Res.*, 2013, **46**, 1517.
15. T. J. Meyer, M. H. V. Huynh and H. H. Thorp, *Angew. Chem. Int. Ed.*, 2007, **46**, 5284.
16. E. F. Pettersen, T. D. Goddard, C. C. Huang, G. S. Couch, D. M. Greenblatt, E. C. Meng and T. E. Ferrin, *J. Comput. Chem.*, 2004, **25**, 1605.
17. Y. Zhang, K. de La Harpe, A. A. Beckstead, L. Martínez-Fernández, R. Improta and B. Kohler, *J. Phys. Chem. Lett.*, 2016, **7**, 950.
18. Y. Zhang, X.-B. Li, A. M. Fleming, J. Dood, A. A. Beckstead, A. M. Orendt, C. J. Burrows and B. Kohler, *J. Am. Chem. Soc.*, 2016, **138**, 7395.
19. K. de La Harpe, C. E. Crespo-Hernández and B. Kohler, *J. Am. Chem. Soc.*, 2009, **131**, 17557.
20. G. W. Doorley, D. A. McGovern, M. W. George, M. Towrie, A. W. Parker, J. M. Kelly and S. J. Quinn, *Angew. Chem. Int. Ed.*, 2009, **48**, 123.
21. L. P. Candeias and S. Steenken, *J. Am. Chem. Soc.*, 1989, **111**, 1094.
22. V. Y. Shafirovich, S. H. Courtney, N. Q. Ya and N. E. Geacintov, *J. Am. Chem. Soc.*, 1995, **117**, 4920.
23. J. D. Gu, J. Wang and J. Leszczynski, *Phys. Chem. Chem. Phys.*, 2016, **18**, 13657.
24. A. Hazra, A. V. Soudackov and S. Hammes-Schiffer, *J. Phys. Chem. B*, 2010, **114**, 12319.
25. B. C. Westlake, M. K. Brennaman, J. J. Concepcion, J. J. Paul, S. E. Bettis, S. D. Hampton, S. A. Miller, N. V. Lebedeva, M. D. E. Forbes, A. M. Moran, T. J. Meyer and J. M. Papanikolas, *Proc. Nat. Acad. Sci. USA*, 2011, **108**, 8554.
26. P. Goyal, C. A. Schwerdtfeger, A. V. Soudackov and S. Hammes-Schiffer, *J. Phys. Chem. B*, 2016, **120**, 2407.
27. R. Jimenez, G. R. Fleming, P. V. Kumar and M. Maroncelli, *Nature*, 1994, **369**, 471.
28. A. Hazra, A. V. Soudackov and S. Hammes-Schiffer, *J. Phys. Chem. Lett.*, 2011, **2**, 36.
29. P. Goyal and S. Hammes-Schiffer, *ACS Energy Lett.*, 2017, **2**, 512.

